

MEASUREMENT AND INTERPRETATION OF PLUTONIUM SPECTRA

J. Blaise*, M. S. Fred, W. T. Carnall,
H. M. Crosswhite and H. Crosswhite

CONF-821265--1

Chemistry Division, Argonne National Laboratory,
9700 South Cass Avenue, Argonne, Illinois 60439 and
*Laboratoire Aimé Cotton CNRS II,
Bat. 505, 91405 Orsay Cedex, France

DE84 003672

The atomic spectroscopic data available for plutonium are among the richest of any in the periodic system. They include high-resolution grating and Fourier-transform spectra as well as extensive Zeeman and isotope-shift studies. We summarize the present status of the term analysis and cite the configurations that have been identified. A least-squares adjustment of a parametric Hamiltonian for configurations of both Pu I and Pu II has shown that almost all of the expected low levels are now known. The use of a model Hamiltonian applicable to both lanthanide and actinide atomic species has been applied to the low configurations of Pu I and Pu II making use of trends predicted by ab initio calculations. This same model has been used to describe the energy levels of Pu³⁺ in LaCl₃, and an extension has permitted preliminary calculations of the spectra of other valence states.

In the fifteen years since publication of an earlier status report on the atomic spectra of plutonium and other actinide elements (1) there has been steady progress, especially in the parametric interpretation of the energy levels. The analogy to lanthanide electronic structure has been more firmly established, the relationships among all the elements of the actinide series have been clarified, and a detailed theory of the lanthanide/actinide crystal spectra has been developed. The most thoroughly advanced of the actinide atomic spectroscopic studies are probably those for plutonium, so it is particularly appropriate that in this 40th anniversary year we look again at where we stand. Because of the close relationship between ionic energy levels in the free state and

DISCLAIMER

This report was prepared as an account of work sponsored by an agency of the United States Government. Neither the United States Government nor any agency thereof, nor any of their employees, makes any warranty, express or implied, or assumes any legal liability or responsibility for the accuracy, completeness, or usefulness of any information, apparatus, product, or process disclosed, or represents that its use would not infringe privately owned rights. Reference herein to any specific commercial product, process, or service by trade name, trademark, manufacturer, or otherwise does not necessarily constitute or imply its endorsement, recommendation, or favoring by the United States Government or any agency thereof. The views and opinions of authors expressed herein do not necessarily state or reflect those of the United States Government or any agency thereof.

HEAVY ELEMENTS RESEARCH GROUP

Chemistry Division

Argonne National Laboratory

MEASUREMENT AND INTERPRETATION OF PLUTONIUM SPECTRA

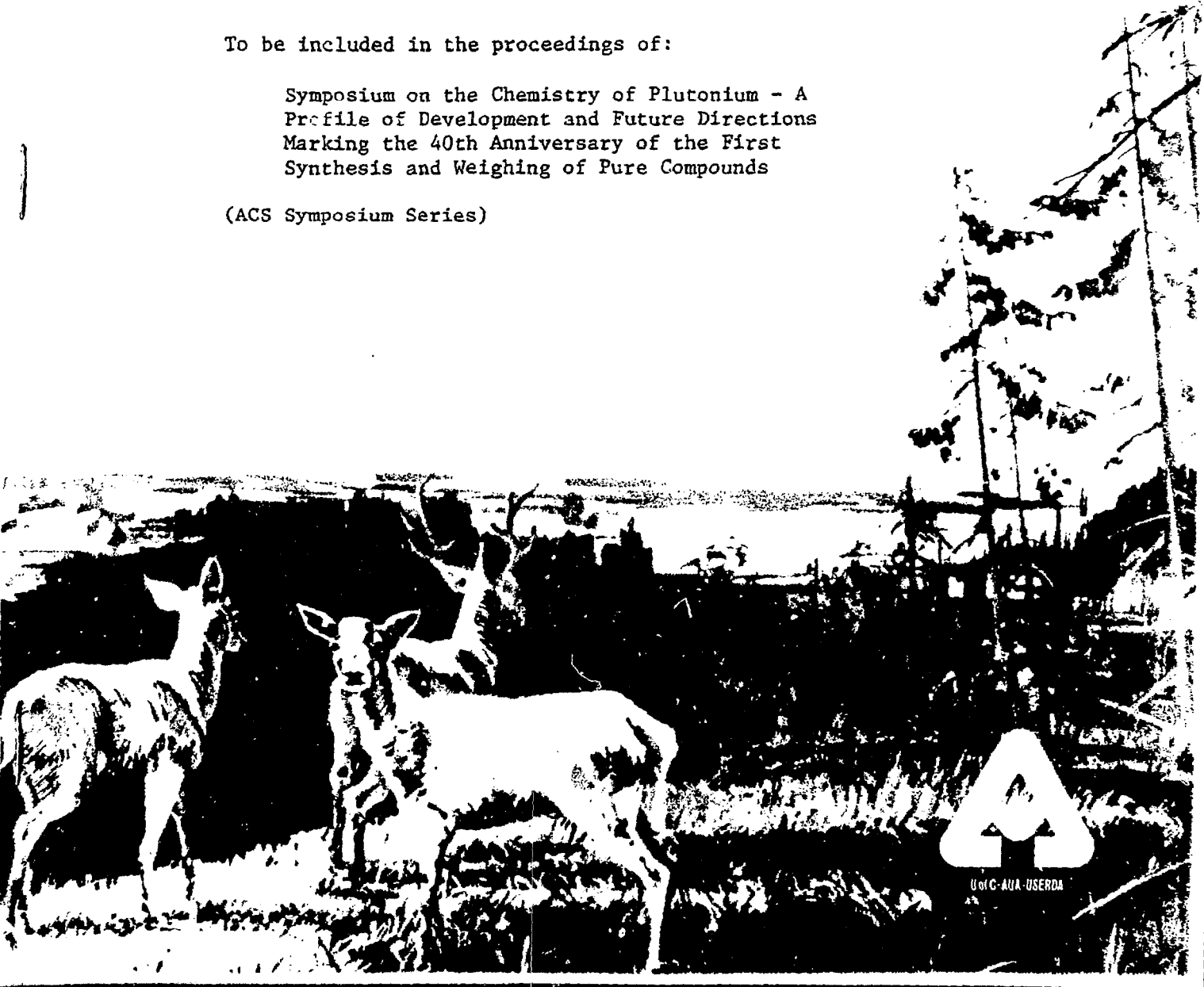
J. Blaise*, M. S. Fred, W. T. Carnall,
H. M. Crosswhite and H. Crosswhite

Chemistry Division, Argonne National Laboratory,
9700 South Cass Avenue, Argonne, Illinois 60439 and
*Laboratoire Aimé Cotton CNRS II,
Bat. 505, 91405 Orsay Cedex, France

To be included in the proceedings of:

Symposium on the Chemistry of Plutonium - A
Profile of Development and Future Directions
Marking the 40th Anniversary of the First
Synthesis and Weighing of Pure Compounds

(ACS Symposium Series)



UofG-AUA-USERDA

in crystalline environments, the current status of both experimental approaches is presented, along with a brief summary of the generalized parametric theory. A more thorough discussion of the results of the term analysis for neutral plutonium (Pu I) will be given elsewhere (2); a complete listing of spectrum lines and energy levels for Pu I and Pu II will be made available as an Argonne National Laboratory Report (3). Abbreviated line lists were recently published by Conway and coworkers (4), and some independent work has also been reported by Striganov (5). Less progress has been made in interpreting the spectra of the higher valence states of plutonium in condensed phases. The summary of studies published up to ~1970 (6) is still a relevant description of the status of this work.

Free-Ion Spectra

The spectrum of Pu was first photographed in 1943 by Rollefson and Dodgen (7), who measured the wavelengths (and intensities) of about 125 lines. However, the first energy level analysis did not come until 1959, when McNally and Griffin (8), using a low-current dc arc loaded with ^{239}Pu in a magnetic field of 2.447 teslas, found 7 out of the 13 levels of the ground terms $5f^6 7s^8 F$ and $^6 F$ in Pu II and also reported 84 high odd levels. (Only 73 of these levels have been confirmed).

The ground multiplet of Pu I was subsequently established by Bovey and Gerstenkorn (9). Combining Harwell Zeeman spectra (from an electrodeless discharge tube containing ^{239}Pu in a magnetic field of 3 teslas (10), with the hyperfine structure and isotope shift measurements made at Laboratoire Aimé Cotton (LAC) from a hollow cathode with a photoelectric Fabry-Perot interferometer, these authors found the lowest five levels of $5f^6 7s^2 ^7 F$, as well as 25 upper odd levels (9, 11). Beginning in 1961, the analysis of the plutonium spectra became a joint project carried out by spectroscopists from three laboratories: Argonne National Laboratory (ANL), Lawrence Livermore National Laboratory (LLNL) and LAC. In the early stages of the term analysis, when separated isotopes became available in sufficient quantity for spectroscopic use, special electrodeless tubes were prepared for particular experiments. One, prepared by E. Worden for LLNL, contained 88% ^{240}Pu for use with the ANL 30-foot Paschen-Runge spectrograph and the 2.4 tesla magnet. The thousands of Zeeman patterns (an example is shown in Fig. 1), obtained with this tube were essential for further progress in the analysis. The small residual amount of ^{239}Pu also permitted isotope-shift measurements to supplement the more accurate interferometric measurements of Gerstenkorn (11) and Striganov and Korostyleva (12, 13, 14). Subsequent spectrograms taken with tubes prepared by F. S. Tomkins at ANL

with mixtures of ^{239}Pu and even isotopes 238-244 (as they became available as separated species) were measured by Gerstenkorn at LAC. In 1970 the spectra of ^{240}Pu and of a mixture of the 240, 242, and 244 isotopes were recorded by Fourier-transform spectroscopy at LAC up to 3.59 μm . A portion of one of these recordings is shown in Fig. 2. The higher resolution made available by these experiments and the connections between low levels made possible by this extension into the infrared greatly advanced the analysis.

For easier reference to earlier work the shift for (239-240) was adopted as a reference for tabulation and where necessary derived from the (240-244) isotope shift by dividing the latter by 2.531, a constant factor determined by Blaise *et al.* (15). Over 9500 isotope shifts have now been measured, 50% of them in the infrared.

The number of energy levels found to date, with the aid of the Zeeman effect and the isotope shift data, is 605 even and 586 odd levels for Pu I and 252 even and 746 odd for Pu II. The quantum number J has been determined for all these levels, the Landé g-factor for most of them, and the isotope shift for almost all of the Pu I levels and for half of those of Pu II. Over 31000 lines have been observed of which 52% have been classified as transitions between pairs of the above levels. These represent 23 distinct electron configurations.

The main problems in these very complex spectra are (1) to find the levels, and (2) to assign the levels to the proper configuration. In the absence of configuration interaction one can estimate the isotope shift for various configurations, taking into account the screening of the 7s electron charge density at the nucleus by the 5f, 6d, and 7p electrons (16). Comparison of these estimates with experimental observations is an important first step in identifying numerical energy levels with their quantum mechanical counterparts. Computations of the central electron density, $[4\pi\psi_s^2(0)]$ have been reported using both the non-relativistic (17) and relativistic (18) Hartree-Fock procedures. When the isotope shift characteristic of the lines belonging to a particular configuration is plotted against the relativistic value for $4\pi\psi_s^2(0)$, the resulting relationship is seen to be a linear function, Fig. 3 (18).

Thus far, we have identified levels belonging to 14 different configurations of Pu I and to 9 configurations in Pu II. The lowest levels of these configurations are given in Table I along with Landé g-factors and the experimental isotope shifts. The latter values are averages and have changed in magnitude somewhat as more experimental data has been analyzed. This can be seen by comparison of values in Table I with earlier tabulations such as shown in Fig. 7 of reference 1. Several levels showing anomalous isotope shifts are perturbed by nearby levels with the same J but which however belong to another configuration. For a more detailed

Table I. The Lowest Level of Each Configuration of Pu I and Pu II with their Corresponding Landé g-Values and Experimental Isotope Shifts (E in cm^{-1} and IS in 10^{-3}cm^{-1}).

Pu I		E	g	IS	Pu I		E	g	IS
$5f^6 7s^2$	$7F_0$	0	-	465	$5f^5 6d 7s^2$	$7K_4^{\circ}$	6314	0.487	653
$5f^6 6d 7s$	$9H_1$	13528	-0.590	253	$5f^5 6d^2 7s$	$9L_4^{\circ}$	14912	0.496	488
$5f^6 6d^2$	$9I_2$	31711	0.200	115	$5f^5 6d^3$	$9L_4^{\circ}$?		
					$5f^5 7s^2 7p$	$7I_3$	17898	0.450	698
$5f^6 7s 7p$	$9G_0^{\circ}$	15449	-	336	$5f^5 6d 7s 7p$	$9L_4$	20828	0.352	467
$5f^6 6d 7p$	$9I_2^{\circ}$	33071	0.673	293	$5f^5 6d^2 7p$	$9M_5$	37415	0.980	403
$5f^6 7s 8s$	$9F_1$	31573	2.403	446	$5f^5 6d 7s 8s$	$9K_3^{\circ}$	39618	0.270	503
$5f^7 7s$	$9S_4^{\circ}$	25192	1.768	273					
					$5f^4 6d^2 7s^2$	$7M_6$	36051	0.830	535
<u>Pu II</u>									
					$5f^5 7s^2$	$6H_5^{\circ}$	8199	0.414	896
$5f^6 7s$	$8F_{1/2}$	0	3.150	381	$5f^5 6d 7s$	$8K_7^{\circ}$	8710	0.308	555
$5f^6 6d$	$8H_{3/2}$	12008	-0.019	77	$5f^5 6d^2$	$8L_9^{\circ}$	17297	0.494	242
					$5f^5 7s 7p$	$8I_{5/2}$	30956	0.646	424
$5f^6 7p$	$8G_{1/2}^{\circ}$	22039	0.344	287	$5f^5 6d 7p$	$8L_9^{\circ}$	33793	0.800	208
$5f^7$	$8S_{7/2}^{\circ}$?		(0)					
					$5f^4 6d^2 7s$	$8M_{11/2}$	37641	0.70	813

discussion of the dependence of isotope shifts on the electron configuration occupancy, see Reference (18). According to the systematic relationships developed by Brewer (19), the still-missing f^{5d^3} configuration in Pu I should begin around $27000 \pm 5000 \text{ cm}^{-1}$, and the level $5f^7(8S_{7/2})$ of Pu II is predicted to occur at $14000 \pm 8000 \text{ cm}^{-1}$.

A further check on the configuration assignments made to date can be obtained by systematically comparing those given in Table I for the lowest levels with analogous ones for other elements, as in Figs. 4 and 5 for all the known actinide configurations. To better see the trends across the series for given configuration types we have changed the energy reference from the experimental zero (ground state) to the lowest level of a particular configuration type. In the left half of Fig. 4, we have chosen $5f^N 7s^2$ as the reference. Configurations with two valence electrons then tend to show a flatter, less irregular display than if referenced against a ground state with variable configuration type. Configurations with three or four valence electrons show a steep, but also more regular, rise as the f-shell collapse progresses. In the alternate display on the right, $5f^{N-1} 6d 7s^2$ lowest levels were taken as the reference. Trivalent configurations are now relatively flat, with the former reference $5f^N 7s^2$ configurations showing a steep fall and $5f^{N-2} 6d^2 7s^2$ a less steep rise. Not all configuration types are plotted in both diagrams. Similar displays of Pu II lowest levels are plotted in Fig. 5, with $5f^N 7s$ and $5f^{N-1} 7s^2$ being chosen for alternative references. All the assignments given in Table I are consistent with these diagrams.

The first and second spectra of plutonium are probably the most thoroughly studied of any in the periodic table insofar as experimental description of the observed spectra and the term analysis is concerned, but a detailed quantum mechanical treatment has been handicapped by their great complexity. Fortunately, the lowest odd and lowest even configurations for both Pu I and Pu II are relatively simple, and parametric studies of the lowest levels of the $5f^6 7s^2$, $5f^5 6d 7s^2$ and $5f^6 7s 8s$ configurations in Pu I (20, 21) and $5f^6 7s$ in Pu II (21) were performed at an early stage. A "generalized" parametric study (22) of the $5f^N 7s^2$ and $5f^N 7s$ configurations in the first and second spectra of the actinides has shown a smooth variation of all the usual parameters of the core $5f^N$. The only missing level below 20000 cm^{-1} in $5f^6 7s^2$ of Pu I has now been found, 107 cm^{-1} lower than predicted.

Some rather heavily-truncated versions of the more complex configurations have been used at ANL to assist in level identifications. A summary of the fitted parametric results for the lowest configurations of Pu I and Pu II is given in Table II. In some cases configuration mixing has been included. The numbers enclosed in parentheses following the

Table II. Parameter Values for Low Plutonium Configurations in cm^{-1} .

	Pu I			Pu II			
	$f^6 s^2$	$f^6 ds$	$f^5 ds^2$	$f^6 s^b$	$f^6 d^a$	$f^5 s^2$	$f^5 ds^a$
EAV	45122(189)	65466(1076)	52342(115)	-	60844(169)	48696(215)	57794(328)
F^2	45114(624)	47578(1373)	[49300]	43311(221)	[43500]	49066(770)	49230(1243)
F^4	31656(1174)	[36164]	[39500]	32103(536)	[34000]	39640(719)	37215(1468)
F^6	[24452]	[27124]	27460(739)	23201(297)	[24000]	26946(785)	[27918]
α	[32.55]	[32.55]	[35]	53.5(1.5)	[31.5]	[32.55]	[32.55]
β	[-652]	[-750]	[-900]	-1261(84)	[-750]	[-652]	[-652]
γ	[1200]	[1300]	[1100]	2635(140)	[1300]	[1200]	[1200]
ζ_f	2063(20)	2100(26)	2233(12)	2079(11)	2084(26)	2275(27)	2263(11)
ζ_d		897(42)	1412(28)		1429(82)		1677(39)
$F^2(\text{fd})$		9469(593)	14973(335)		18805(635)		20468(445)
F^4		11108(987)	[11000]		[12000]		14251(1090)
G^1		3977(202)	6357(113)		2266(594)		9027(159)
G^2		[902]	614(355)		[1000]		387(932)
G^3		9148(638)	8293(304)		10840(823)		9452(528)
G^4		[1000]	[2000]		[1000]		1903(808)
G^5		985(549)	6081(307)		[7500]		8515(661)
$G^3(\text{fs})$		2819(93)		2498(45)			2353(93)
$G^2(\text{ds})$		3684(549)					7838(386)
$R^2(\text{fd,fs})$	-8260(1715) ^c					-6135(508) ^c	
$R^3(\text{fd,sf})$	-3782(1291)					-564(537)	

^a Also: $T_2^2 = 200$, $T_4^3 = 30$, $T_4^4 = 11$, $T_6^6 = -368$, $T_7^7 = 389$, $T_8^8 = 352$, $M^0 = 0.75$, $M^2 = 0.41$, $M^4 = 0.29$,
 $P^2 = 1334$, $P^4 = 1000$, $P^6 = 667$, all fixed.

^b From Reference 22.

^c Configuration mixing between $f^N s^2$ and $f^N ds$.

tabulated values represent the statistical errors associated with that particular parameter value. A number enclosed by square brackets is one for which that parameter was held fixed during the least-squares fitting procedure. Calculations such as these have been invaluable in defining the quantum-electronic nature of the empirical levels; the derived eigenvectors are used to compute g-values and isotope shifts for direct comparison with experimental measurements as well as for more indirect analyses of hyperfine structure parameters (23). Because of the stability of the f-orbitals it is possible to draw a strong parallel among their atomic parameters and analogous parameters from studies of other actinide and lanthanide cases. In fact, Hartree-Fock calculations of the associated radial integrals shown in Tables IIIA and B for some cases of interest here, together with appropriate systematic corrections deduced from empirical studies, can be used as the basis of a parametric model which embraces all of the actinide and lanthanide spectra so far subjected to detailed study. These corrections take two forms: (1) a numerical correction to the Hartree-Fock estimates, partially accounting for the masking of parameters which is one consequence of the breakdown of the single-configuration approximation and (2) introduction of additional (effective) Hamiltonian operators which have no meaning in a single-configuration approximation but which to a large extent mimic the effects of interactions with other configurations without increasing the sizes of the matrices involved. Because these corrections to the Hartree-Fock estimates, and the empirical parameters associated with effective operators, are nearly independent of the particular ion under study, it is possible to make reasonably accurate estimates of plutonium parameters in advance of the detailed analysis. Indeed, as nearly as we have been able to determine, none of the effective-operator parameters are significantly different in analogous crystal/free-ion comparisons. As a consequence, we have used the general parametric model to give estimates where empirical data are insufficient, in attempts to interpret both crystal and free-ion cases. In spite of the complications brought about by the effects of the crystal-field interaction, the fact that in crystal spectra only transitions between levels of $5f^N$ itself are encountered at low energies has led to a great simplification of the problems of identification and interpretation. The condensed-phase spectra of plutonium in the tetravalent, (IV), through (VII) oxidation states are known, but theoretical interpretation of the observed transitions is not as highly developed as that characteristic of Pu^{3+} . However, several general statements regarding the electronic structure of Pu in condensed phase can be made as a result of recent work. The subsequent discussion, therefore, represents a continuation of that of Pu I and Pu II spectra,

Table III(A). HFR^a Values for 5f^N Cores of Pu Configurations.

Spectrum	Configuration	F ²	F ⁴	F ⁶	ζ	M ⁰
I	5f ⁶ 7s ²	71461	46094	33638	2230	0.75
	5f ⁵ 6d7s ²	76279	49543	36268	2422	0.84
	5f ⁶ 6d7s	70790	45619	33280	2215	0.74
II	5f ⁶ 7s	71900	46400	33867	2239	0.76
	5f ⁵ 7s ²	77274	50260	36815	2249	0.86
	5f ⁵ 6d7s	76452	49664	36360	2426	0.85
	5f ⁶ 6d	70980	45747	33374	2217	0.74
III	5f ⁶	72563	46868	34220	2255	0.77
	5f ⁵ 6d	76820	49926	36558	2436	0.85
IV	5f ⁵	78223	50942	37335	2479	0.88
V	5f ⁴	82908	54356	39965	2679	0.98
VI	5f ³	86982	57347	42285	2914	1.09
VII	5f ²	90625	60037	44381	3130	1.19

^aComputed using Hartree-Fock methods and including an approximate relativistic correction (24).

Table III(B). HFR^a Values for Inequivalent-Electron Interactions

Parameter	Pu I	Pu I	Pu II	Pu II	Pu III
	5f ⁵ 6d7s ²	5f ⁶ 6d7s	5f ⁵ 6d7s	5f ⁶ 6d	5f ⁵ 6d
ζ _d	1695	985	1976	1418	2255
F ² (fd) ^d	24469	17687	27225	22959	29649
F ⁴ (fd)	12649	8871	14292	11913	15773
G ¹ (fd)	14187	11109	15918	14713	17378
G ³ (fd)	10326	7588	11701	10257	12918
G ³ (fs)		2995	3696		
G ² (ds)		19822	21708		

^aComputed using Hartree-Fock methods and including an approximate relativistic correction (24).

beginning with consideration of divalent plutonium, and addressing the condensed-phase spectra at increasing stages of ionization.

Crystal Spectra

In what follows we briefly review some of the previous attempts to analyze the available spectra of plutonium (6). In addition, we estimate energy level parameters that identify at least the gross features characteristic of the spectra of plutonium in various valence states in the lower energy range where in most cases, several isolated absorption bands can be discerned. The method used was based on our interpretation of trivalent actinide and lanthanide spectra, and the generalized model referred to earlier in the discussion of free-ion spectra.

As was the case with lanthanide crystal spectra (25), we found that a systematic analysis could be developed by examining differences, ΔP , between experimentally-established actinide parameter values and those computed using Hartree-Fock methods with the inclusion of relativistic corrections (24), as illustrated in Table IV for An^{3+} . Crystal-field effects were approximated based on selected published results. By forming tabulations similar to Table IV for 2^+ , 4^+ , 5^+ and 6^+ spectra, to the extent that any experimental data were available to test the predictions, we found that the ΔP -values for Pu^{3+} provided a good starting point for approximating the structure of plutonium spectra in other valence states. However, adjustments were required for each individual oxidation state.

In addition to transitions within the $5f^N$ configuration which characterize the lower energy states in the following discussion, the energy of onset of $f \rightarrow d$ transitions is an important variable which strongly influences the nature of the spectra. For example, intense absorption bands characteristic of $f \rightarrow d$ transitions in the ultraviolet range of the $Pu^{3+}(\text{aquo})$ spectrum, Fig. 6, completely mask the presence of weaker $f \rightarrow f$ transitions. The first $f \rightarrow d$ transition is shifted toward higher energies with increasing valency, and with increasing atomic number within a single oxidation state.

Prediction of the energy level structure for Pu^{2+} ($5f^6$) is of particular interest since no spectra for this valence state of Pu have been reported. On the basis of what is known of the spectra of Am^{2+} (26), Cf^{2+} (27), and Es^{2+} (28), there appears to be evidence for a very small crystal-field splitting of the free-ion levels. Such evidence encourages use of a free-ion calculation in this particular case. The parameter values selected are indicated in Table V. Based on the systematics given by Brewer (19), the first $f \rightarrow d$ transition should occur near 11000 cm^{-1} , so the $f \rightarrow f$ transitions at higher energies would be expected to be at least partially obscured. A

Table IV. Comparison of Energy Level Parameters Computed Using Hartree-Fock Methods and Those Evaluated from Fitting Experimental Data for An^{3+} (all in cm^{-1}).

	U	Np	Pu	Am
F^2 (HFR) ^a	71442	74944	78223	81346
F^2 (FIT) ^b	<u>39715</u>	<u>44907</u>	<u>48670</u>	<u>51800</u>
ΔP	31727	30037	29553	29546
F^4 (HFR)	46370	48733	50942	53044
F^4 (FIT)	<u>33537</u>	<u>36918</u>	<u>39188</u>	<u>41440</u>
ΔP	12833	11815	11754	11604
F^6 (HFR)	33981	35684	37335	38905
F^6 (FIT)	<u>23670</u>	<u>25766</u>	<u>27493</u>	<u>30050</u>
ΔP	10248	9918	9842	8855
ζ (HFR)	1898	2182	2479	2792
ζ (FIT)	<u>1623</u>	<u>1938</u>	<u>2241</u>	<u>2580</u>
ΔP	275	244	238	212

^aComputed using Hartree-Fock methods and including an approximate relativistic correction (24).

^bComputed by fitting to experimental data.

Table V. Estimated Values of $\Delta F = F^k(\text{or } \zeta)_{\text{HFR}}^a - F^k(\text{or } \zeta)_{\text{EXPT}}^b$ for Pu (all in cm^{-1}).

	Pu ²⁺	Pu ⁴⁺	Pu ⁵⁺	Pu ⁶⁺
ΔF^2	26500	28000	30000	30000
ΔF^4	14000	13000	15000	16000
ΔF^6	10000	9200	10000	11000
$\Delta \zeta$	200	350	350	350

^aThe values of $F^k(\text{or } \zeta)_{\text{HFR}}$ are given in Table IIIA.

^bIn each case the following additional free-ion parameters were included in the calculation, (25): $\alpha = 35$, $\beta = -1000$, $\gamma = 1200$, $T^2 = 200$, $T^3 = 50$, $T^4 = 100$, $T^6 = -300$, $T^7 = 400$, $T^8 = 350$, $P^2 = 1200$, $P^4 = 900$, $P^6 = 600$, $M^0 = .767$, $M^2 = .423$, $M^4 = .293$, all in cm^{-1} .

predicted energy level scheme is given in Fig. 7. The group of bands computed to lie near 10000 cm^{-1} may be useful in any effort to characterize compounds in which this valence state is stabilized.

The spectra of $\text{Pu}^{3+}:\text{LaCl}_3$ (29) and isostructural PuCl_3 (30) have been examined and the energy-level analysis has been refined using extensive crystal-field data. Consequently, the results included in Table IV are well established. As already indicated, they serve as one basis for estimating parameters for higher-valent species.

Attempts have been made to analyze the energy level structure of Pu^{4+} compounds in terms of a free-ion model, but, with increasing metal-ion valence the crystal-field splitting also increases significantly. Frequent overlap in energies of crystal-field levels belonging to several different parent free-ion states is predicted. For a realistic calculation, the crystal-field must be diagonalized simultaneously with the free-ion parts of the interaction. In addition, many Pu^{4+} compounds exhibit an inversion symmetry at the Pu^{4+} site. In such cases the spectrum is dominated by vibronic transitions. The zero-phonon transitions are forbidden in the limit of inversion symmetry but may appear weakly if there is any significant distortion away from the symmetry. Thus, not only must the effects of the crystal-field interaction be treated simultaneously with the free-ion interactions, but the analysis can be exceedingly complex.

There is an interesting similarity in the character of the solution absorption spectra of the isoelectronic ions Np^{3+} and Pu^{4+} even though the absorption bands in Pu^{4+} are all shifted toward higher energies due to increases in both the electrostatic (F^k) and spin-orbit (ζ) parameters, Table VI. We have also examined the spectra of complex alkali-metal: Pu(IV)

fluorides (31), and find a strong similarity in the energies at which many of the absorption bands are observed compared to those for $\text{Pu}^{4+}(\text{aquo})$. Thus, while the crystal-field interaction of An^{4+} is larger than that in An^{3+} , some of the characteristics of the latter structure still remain.

Table VI. Estimated Values of Energy Level Parameters for Parametric Model, in cm^{-1} .

	Np^{3+}	Pu^{4+}	Increase
F^2	44900	55000	+22%
F^4	36900	41300	+12%
F^6	25770	30800	+20%
ζ	1938	2350	+21%

The electrostatic and spin-orbit parameters for Pu^{4+} which we have deduced are similar to those proposed by Conway some years ago (32). However, inclusion of the crystal-field interaction in the computation of the energy level structure, which was not done earlier, significantly modifies previous predictions. As an approximation, we have chosen to use the crystal-field parameters derived for Cs_2UCl_6 (33), Table VII, which together with the free-ion parameters lead to the prediction of a distinct group of levels near 1100 cm^{-1} . Of course a weaker field would lead to crystal-field levels intermediate between 0 and 1000 cm^{-1} . Similar model calculations have been indicated in Fig. 8 for Np^{4+} , Pu^{4+} and Am^{4+} compared to the solution spectra of the ions. For Am^{4+} the reference is Am^{4+} in 15 M NH_4F solution (34).

Table VII. Crystal-Field Parameters for Hexahalide $5f^1$ -Actinide Ions.

	$\text{Cs}_2\text{UCl}_6(5f^2)^a$	$\text{CsUF}_6(5f^1)^b$	$\text{NpF}_6(5f^1)^c$
B_0^4	7200 cm^{-1}	22500 cm^{-1}	44550 cm^{-1}
B_0^6	1300 cm^{-1}	3500 cm^{-1}	8000 cm^{-1}

^aCrystal-field parameters are from Reference 33, consistent with those for $\text{Pa}^{4+}:\text{Cs}_2\text{ZrCl}_6(5f^1)$ (43).

^bReference 40.

^cPresent work.

It should be emphasized that whereas the theoretical modelling of An^{3+} spectra in the condensed phase has reached a high degree of sophistication, the type of modelling of electronic structure of the (IV) and higher-valent actinides discussed here is restricted to very basic interactions and is in an initial state of development. The use of independent experimental methods for establishing the symmetry character of observed transitions is essential to further theoretical interpretation just as it was in the trivalent ion case.

For valence states higher than (IV), two types of Pu compounds are known: the simple and complex halides, such as PuF_6 and $CsPuF_6$, and the plutonyl species, PuO_2^{2+} or PuO_2^{++} . The oxygenated species are encountered in aqueous solutions. However, definitive analyses of the latter type spectra including that characteristic of Pu(VII) have yet to be proposed. The difficulty in analyzing the spectra of plutonyl compounds (35), is not unique; some degree of controversy still surrounds the interpretation of the spectra of UO_2^{2+} (36). In the spirit of the present paper, our interests were to explore some of the consequences of a predictive model for energy level structures. At present such model calculations are best suited for the spectra of the halides.

Spectroscopic analysis of Pu^{5+} and Pu^{6+} halides is in its initial stages. No low-temperature single-crystal spectra have been reported. A 25°C mull spectrum of the compound Rb_2PuF_7 was described earlier (37), and is now supplemented by the results for $CsPuF_6$ (31); PuF_6 gas-phase spectra have been reported by several different groups at ANL (38-39).

One of the methods of estimating the energy level parameters for Pu^{5+} in compounds such as $CsPuF_6$ is to examine the magnitude of the free-ion and crystal-field parameters in other similar An^{5+} compounds. Although there are problems with some of the assumptions that have been made in analyzing the spectra of compounds such as $CsUF_6(5f^1)$ (40-41) and $CsNpF_6(5f^2)$ (42), we tentatively conclude that the approximate crystal field parameters for $CsPuF_6$ represent a reasonable step in the progression of $5f^1$ parameters indicated in Table VII. The actual crystal field in $CsPuF_6$ may be smaller than in $CsUF_6$, and consistent with results reported for $CsNpF_6$. It may also be of lower symmetry. We choose here to use what we believe to be a limiting case for illustration.

The assumption of a large crystal-field interaction for Pu^{5+} spectra makes it necessary to conclude that while certain aspects of earlier free-ion estimates (37) are valid, the "assignment" of free-ion states to observed absorption bands was premature. Much of the structure must be due to crystal-field components of many free-ion groups that overlap in energy or to vibronic satellites similar to those encountered in Cs_2UCl_6 (33). Thus, while the present computations would agree with earlier work in interpreting the levels observed in

Rb₂PuF₇ as well as in CsPuF₆ in the range 6000-7000 cm⁻¹ as belonging to a somewhat isolated first excited state, a more detailed calculation including the CsUF₆ crystal-field gives the results shown in Fig. 9. It predicts an essentially continuous level structure at energies >8800 cm⁻¹. Extensive detailed analysis will be required before firm assignments can be made. However, it should be somewhat more straight-forward to uniquely establish the crystal field splitting of the ground state by observation of fluorescence from the first excited state (~7000 cm⁻¹).

Finally, the highest valence state reported for plutonium in a non-oxygen-containing compound is exemplified in PuF₆, whose optical spectrum has been shown to be extremely complex (39). Estimated free-ion, Table V, and ligand-field parameters used in the present analysis are consistent with those reported earlier (44), but differ considerably from the free-ion parameters developed by Boring and Hecht (45) whose values for F⁴ and F⁶ would appear to us to be distorted. The crystal-field parameters characteristic of NpF₆, Table VII, should represent a good basis for estimating the similar interaction in PuF₆. Our results are summarized in Fig. 10.

Recent observations of fluorescence in NpF₆ and PuF₆ (46) are consistent with the energy-level scheme proposed. However, comparison of the calculated level structure with high-resolution spectra of PuF₆ (44) confirms that much of the observed structure is vibronic in character, built on electronic transitions that are forbidden by the inversion symmetry at the Pu site.

Conclusion

The investigation of Pu free-ion spectra has reached a point at which further progress is slow because of the time-consuming analysis required and incompleteness of the data. In one sense the first phase of this work is complete and rests on the existing extensive experimental data base (3). The possibilities now exist for taking much higher resolution spectra using Fourier-transform methods, but the earlier spectra obtained photographically using high dispersion spectrographs will continue to be an essential building block. The complexity of the interpretive problem, given the many interacting configurations, insures that challenging problems in theory as well as experiment remain to be addressed.

It is also apparent that there remains much to be done in developing our understanding of the model interactions that best characterize the spectra of higher-valent Pu compounds and indeed of the actinides in general. The synthesis of new compounds with a variety of different site symmetries could be of particular value in developing more detailed crystal-field

models. Of equal importance with the theoretical tools is the acquisition of high-resolution spectra under conditions that permit the independent experimental definition of properties that will help characterize the observed transitions. It is the lack of a solid experimental basis that has inhibited more widespread interest in the theoretical modelling.

Literature Cited

1. Fred, M. Adv. Chem. Ser. 1967, 71, 180-202.
2. Blaise, J.; Fred, M.; Gutmacher, R. J. Opt. Soc. Am. (to be submitted).
3. Fred, M.; Blaise, J. Argonne National Laboratory Report, 1983, in preparation.
4. Conway, J. G.; Blaise, J.; Verges, J. Spectrochimica Acta 1976, 31B, 31-47; Conway, J. G. "Handbook of Chemistry and Physics", Weast, R. C.; Astle, M. J., Eds. CRC Press, Boca Raton, 1980, pp. E-290-1.
5. Striganov, A. R., Report IAE-2965, Kurchatov Institute of Atomic Energy, Moscow, 1978 (in Russian). Translated by G. V. Shalimoff, Lawrence Berkeley Laboratory.
6. Carnall, W. T. "Gmelin Handbook of Inorganic Chemistry", Transurane A-2 (Erg.-Werk Band 8) Verlag Chemie, Weinheim/Bergstr., 1973, 35-79.
7. Rollefson, G. K.; Dodgen, H. W. "Report on Spectrographic Analysis Work CK-812", July 1943 (Declassified 29 December 1954).
8. McNally Jr., J. R.; Griffin, P. M. J. Opt. Soc. Am. 1959, 49, 162-6.
9. Bovey, L.; Gerstenkorn, S. J. Opt. Soc. Am. 1961, 51, 522-5.
10. Bovey, L.; Ridgeley, A. "The Zeeman Effect of Pu I", A.E.R.E.-R3393, Harwell, 1960.
11. Gerstenkorn, S. Ann Physique (Paris) 1962, 7, 367-404.
12. Striganov, A. R.; Korostyleva, L. A.; Dontsov, Yu, P. Zh. Eksp. Teor. Fiz. 1955, 28, 480; Sov. Phys. JETP 1955, 1, 354.
13. Korostyleva, L. A. Opt. i. Spektroskopiya 1963, 14, 177; Opt. Spectrosc. (USSR) 1963, 14, 93.
14. Korostyleva, L. A.; Striganov, A. R. Opt. i. Spektroskopiya 1966, 20, 545-53; Opt. Spectrosc. (USSR) 1966, 20, 309-17.
15. Blaise, J.; Fred, M.; Gerstenkorn, S.; Tomkins, F. S. 2nd E.G.A.S. Conference, Hanover, 14-17 July 1970.
16. Blaise, J.; Steudel, A. Z. Physik 1968, 209, 311-28.
17. Wilson, M. Phys. Rev. 1968, 176, 58-63.
18. Rajnak, K.; Fred, M. J. Opt. Soc. Am. 1977, 67, 1314-23.
19. Brewer, L. J. Opt. Soc. Am. 1971, 61, 1101-11, 1666-82.
20. Blaise, J.; Fred, M.; Gerstenkorn, S.; Judd, B. R. C. R. Acad. Sci. Paris 1962, 255, 2403-5.

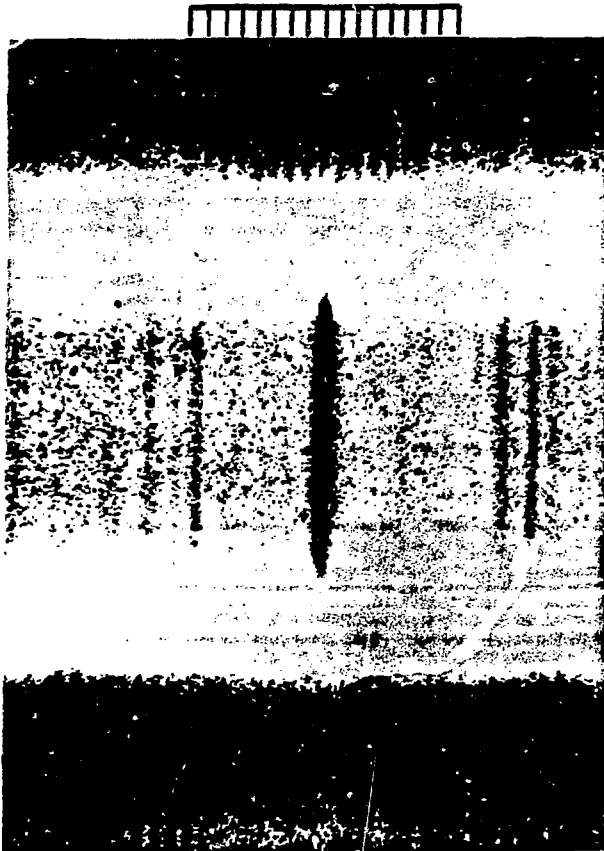
21. Bauche, J.; Blaise, J.; Fred, M. C. R. Acad. Sci. Paris 1963, 256, 5091-93; 257, 2260-63.
22. Blaise, J.; Wyart, J. F.; Conway, J. G.; Worden, E. F. Physica Scripta 1980, 22, 224-30.
23. Bauche-Arnoult, C.; Gerstenkorn, S.; Verges, J.; Tomkins, F. S. J. Opt. Soc. Am. 1973, 63, 1199-1203.
24. Cowan, R. D.; Griffin, C. D. J. Opt. Soc. Am. 1976, 66, 1010-14.
25. Crosswhite, H. M. Colloques Internationaux du C.N.R.S., Spectroscopie des Elements de Transition et des Elements Lourds des Solids, 28 Juin - 3 Juillet 1976, Editions du C.N.R.S., Paris 1977, 65-69.
26. Edelstein, N.; Easley, W.; McLaughlin, R. Adv. Chem. Ser. 1967, 71, 203-10.
27. Peterson, J. R.; Fellows, R. L.; Young, J. P.; Haire, R. G. Radiochem. Radioanal. Letters 1977, 31, 277-82.
28. Fellows, R. L.; Peterson, J. R.; Young, J. P.; Haire, R. G. "The Rare Earths in Modern Science and Technology", McCarthy, G. J.; Rhyne, J. J., Eds. Plenum Corp., New York 1978, 493-99.
29. Conway, J. G.; Rajnak K. J. Chem. Phys. 1966, 44, 348-54; Hessler, J. P.; Carnall, W. T. ACS Sympos. Ser. 1980, 131, 349-68.
30. Carnall, W. T.; Fields, P. R.; Pappalardo, R. G. J. Chem. Phys. 1970, 53, 2922-38.
31. Morss, L. R.; Williams, C. W.; Carnall, W. T. Chapter _____ in this book.
32. Conway, J. G. J. Chem. Phys. 1964, 41, 904-5.
33. Johnston, D. R.; Satten, R. A.; Schreiber, C. L.; Wong, E. Y. J. Chem. Phys. 1966, 44, 3141-3.
34. Asprey, L. B.; Penneman, R. A. Inorg. Chem. 1962, 1, 134-36.
35. Einstein, J. C.; Pryce, M. H. L. Proc. Roy. Soc. 1956, A238, 31-45; J. Res. Natl. Bureau Stds. 1966, 70A, 165-73.
36. Carnall, W. T. "Gmelin Handbook of Inorganic Chemistry", 8th Ed., System 55, Springer-Verlag, Berlin, 1982, 147-57.
37. Varga, L. P.; Reinfeld, M. J.; Asprey, L. B. J. Chem. Phys. 1970, 53, 250-55.
38. Weinstock, B.; Malm, J. G. J. Inorg. Nucl. Chem. 1956, 2, 380-94.
39. Steindler, M. J.; Gunther, W. H. Spectrochim. Acta 1964, 20, 1319-22.
40. Reinfeld, M. J.; Crosby, G. A. Inorg. Chem. 1965, 4, 65-70.
41. Leung, A. F. J. Phys. Chem. Solids 1977, 38, 529-32.
42. Hecht, H. G.; Varga, L. P.; Lewis, W. B.; Boring, A. M. J. Chem. Phys. 1979, 70, 101-108; Poon, Y. M.; Newman, D. J. Chem. Phys. 1982, 77, 1077-79.

43. Axe, J. D. "Electronic Structure of Octahedrally Coordinated Protactinium(IV) in Cs_2ZrCl_6 ", UCRL-9293, Berkeley, 1960.
44. Kugel, R.; Williams, C.; Fred, M.; Malm, J. G.; Carnall, W. T.; Hindman, J. C.; Childs, W. J; Goodman, L. S. J. Chem. Phys. 1976, 65, 3486-92.
45. Boring, M.; Hecht, H. G. J. Chem. Phys. 1978, 69, 112-16.
46. Beitz, J. V.; Williams, C. W.; Carnall, W. T., Chapter _____ in this book.

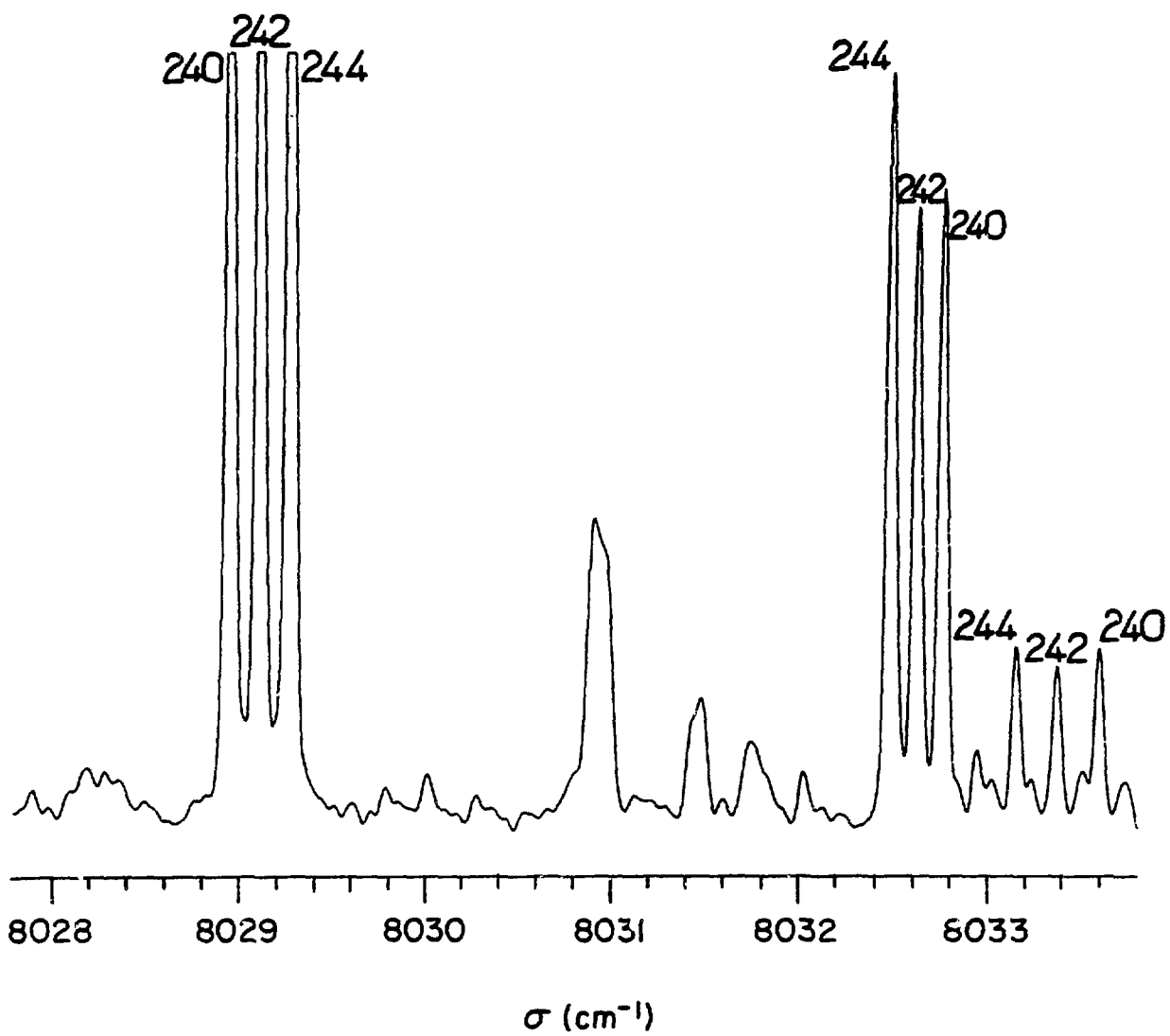
Figure Captions

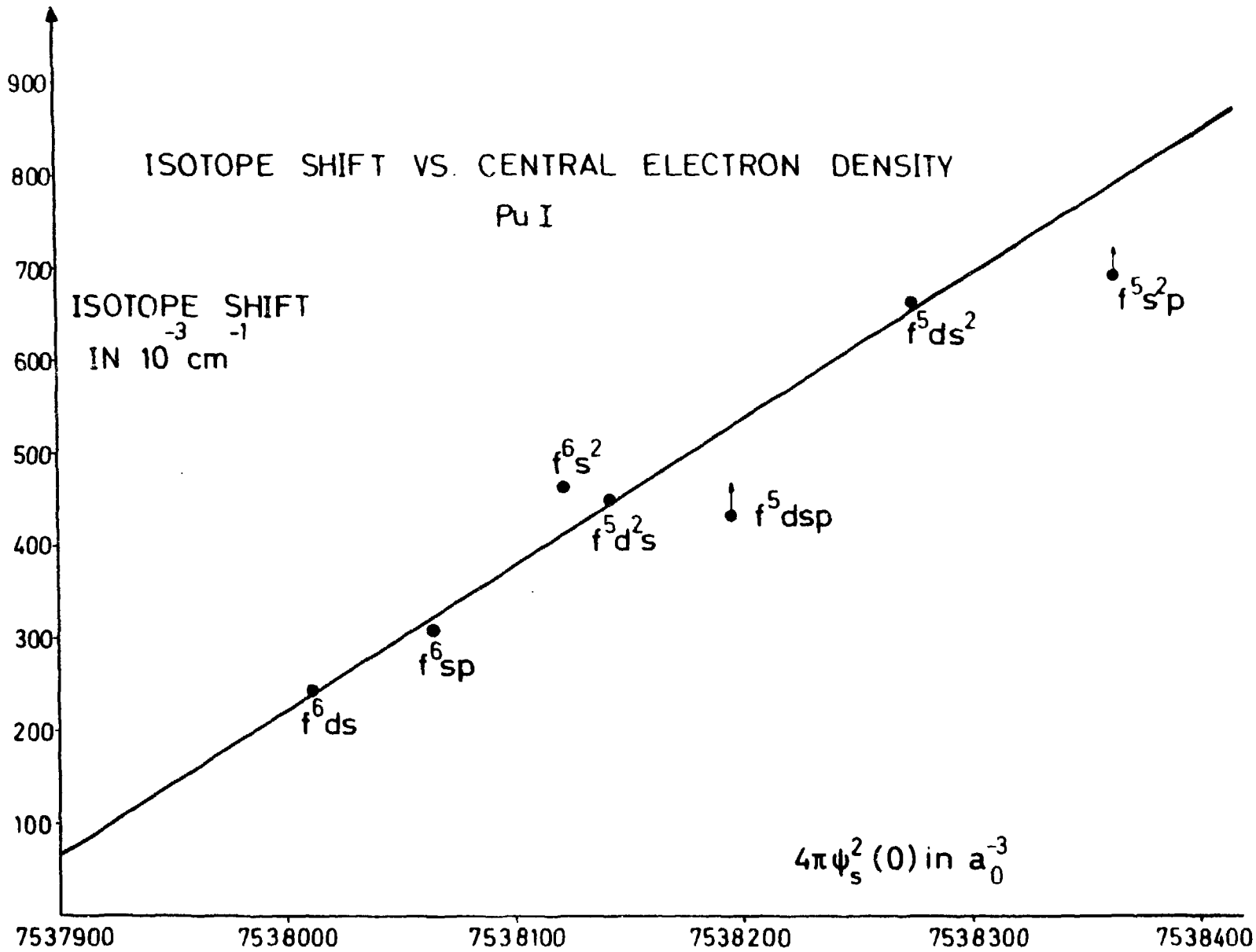
1. Zeeman pattern for Pu I at 8534 \AA photographed at 2.4 teslas.
2. Spectra of a mixture of $^{240,242,244}\text{Pu}$ isotopes recorded by Fourier-transform spectroscopy.
3. Isotope shift for various configurations in Pu I plotted as a function of the central electron density, $4\pi\psi_s^2(0)$.
4. Systematic variation of the lowest-energy levels in a given configuration for An I plotted as a function of N , where $N = Z - 88$.
5. Systematic variation of the lowest-energy levels in a given configuration for An II plotted as a function of N , where $N = Z - 88$.
6. Solution absorption spectra of $\text{U}^{3+}(\text{aquo})$ through $\text{Am}^{3+}(\text{aquo})$ in the region $0\text{-}50000 \text{ cm}^{-1}$.
7. Predicted free-ion energy levels in the $5f^N$ -configuration of U^{2+} through Am^{2+} and the overlapping range of the $5f^N \rightarrow 5f^{N-1}d$ transitions.
8. Solution absorption spectra for Np^{4+} , Pu^{4+} , and Am^{4+} in the range $0\text{-}30000 \text{ cm}^{-1}$ with predicted energy level structure indicated.
9. Predicted energy-level structure for CsUF_6 , CsNpF_6 , and CsPuF_6 in the range $0\text{-}20000 \text{ cm}^{-1}$.
10. Predicted energy-level structure for NpF_6 , PuF_6 , and AmF_6 in the range $0\text{-}18000 \text{ cm}^{-1}$.

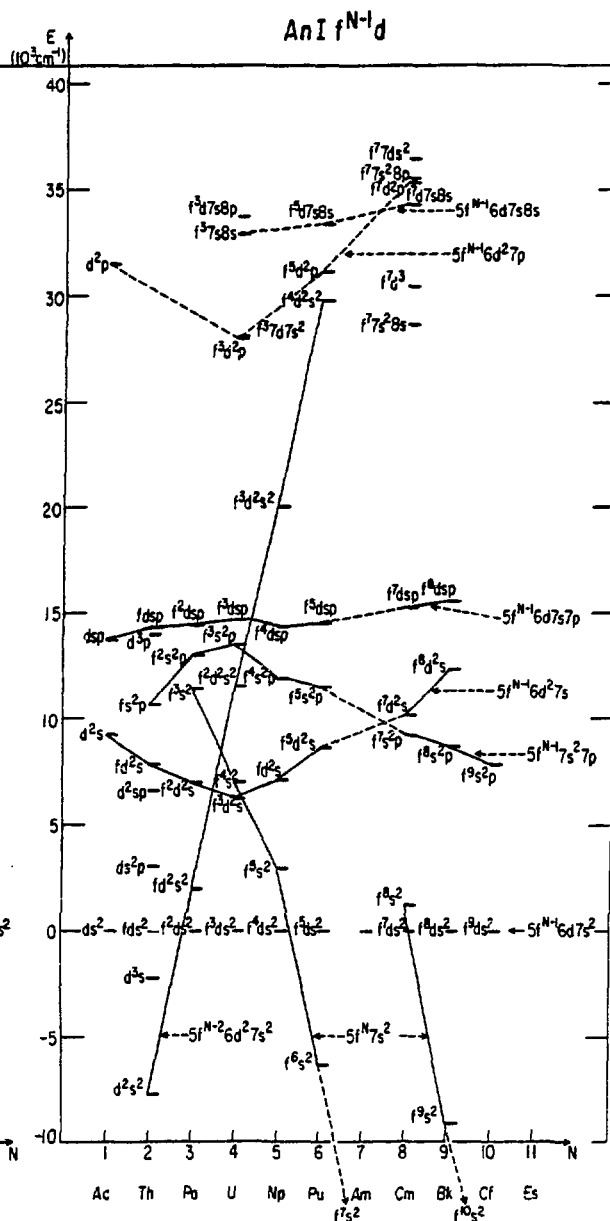
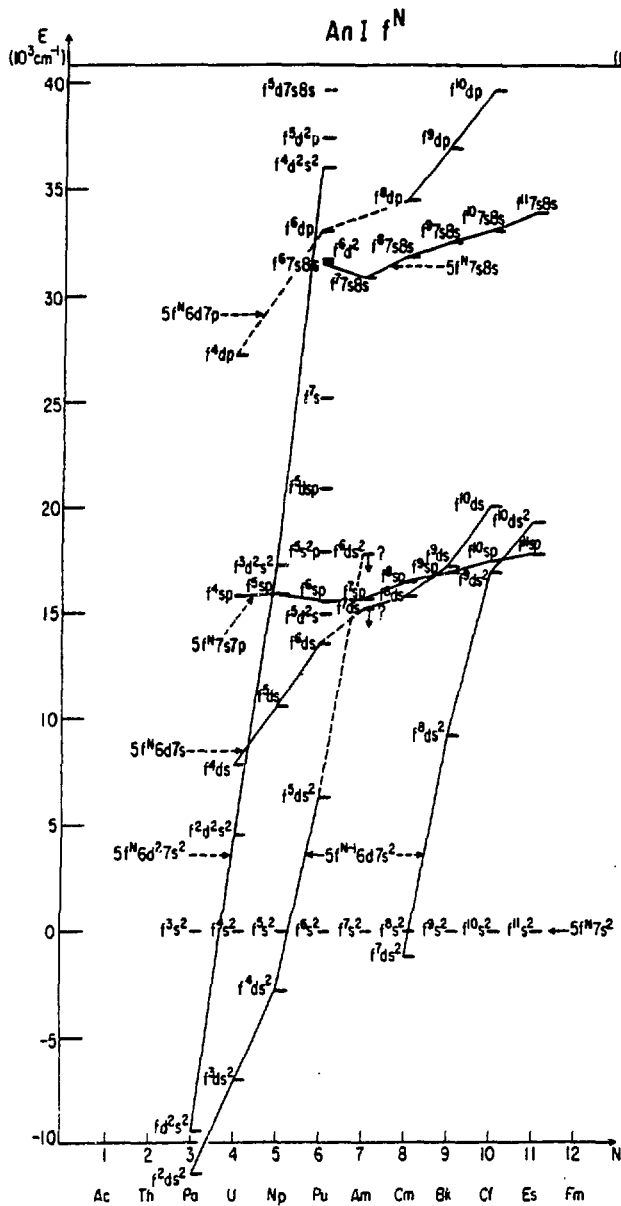
π

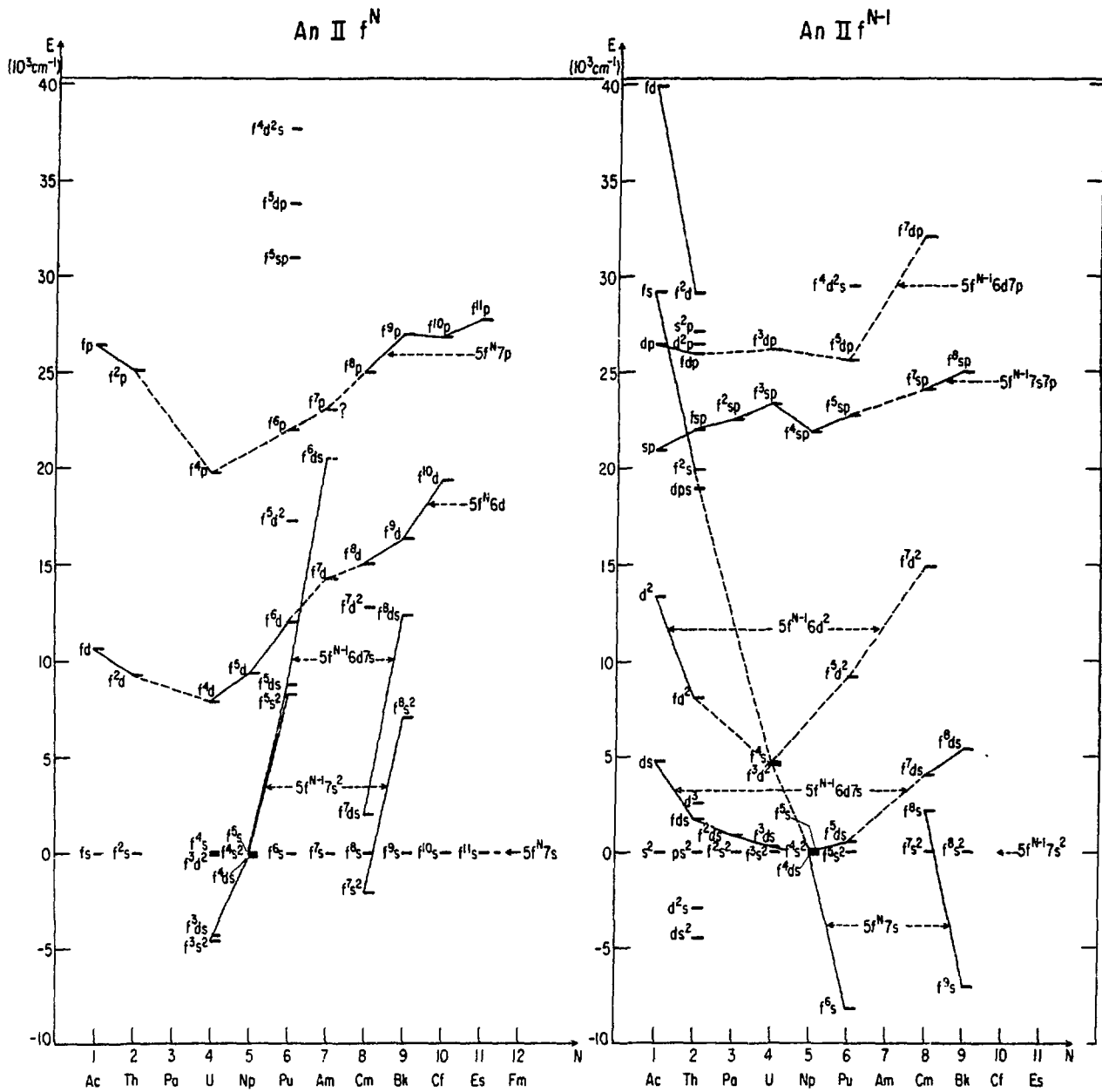


σ









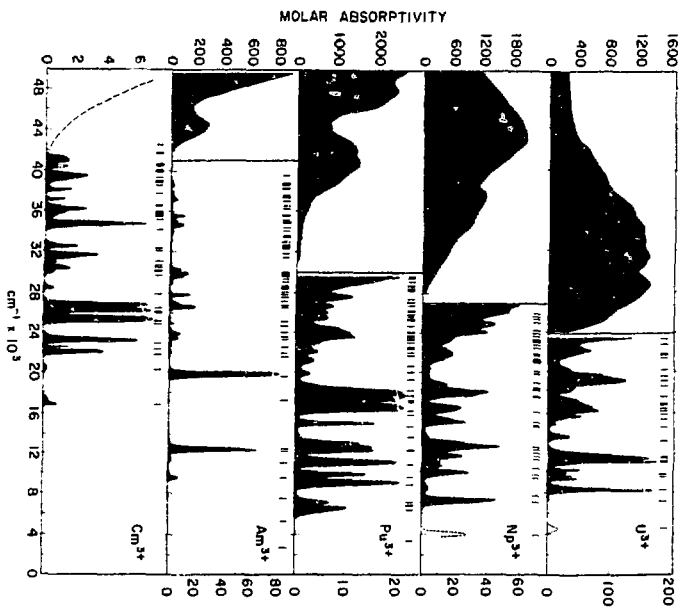


Fig. 6.

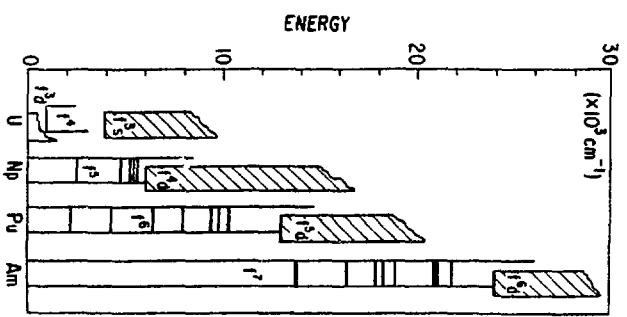
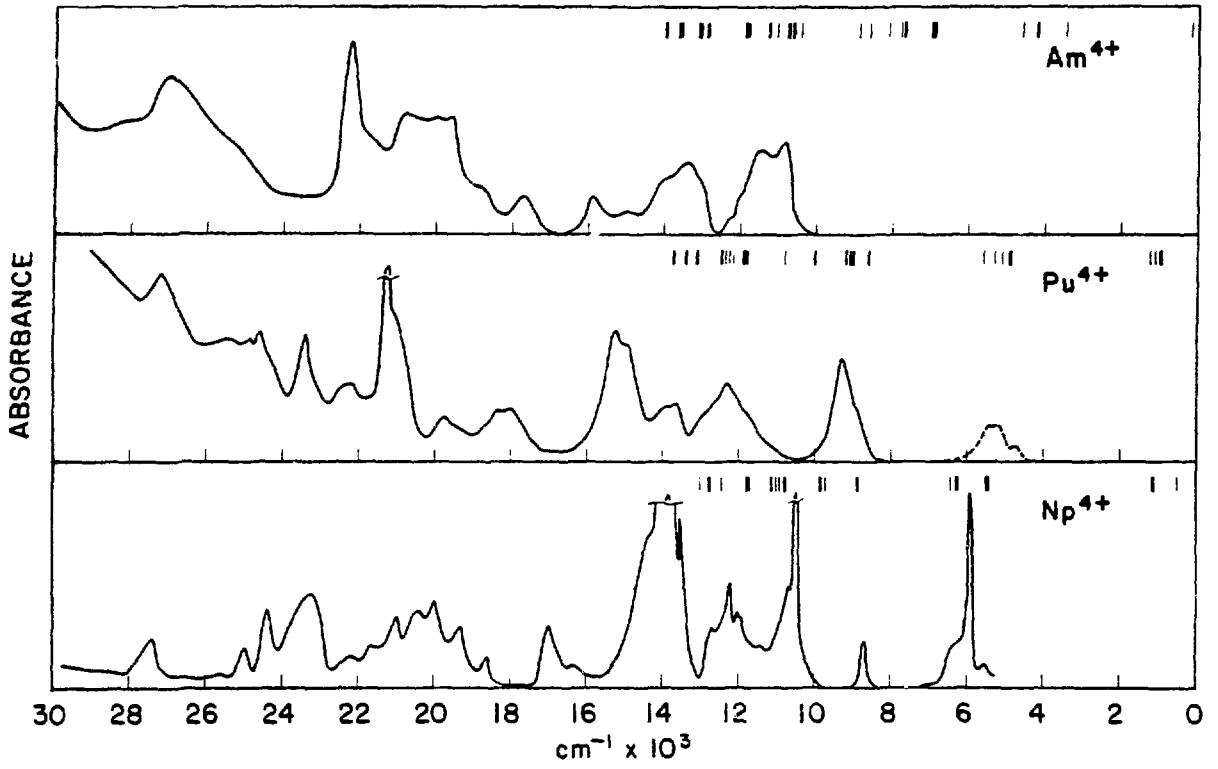


Fig. 7.



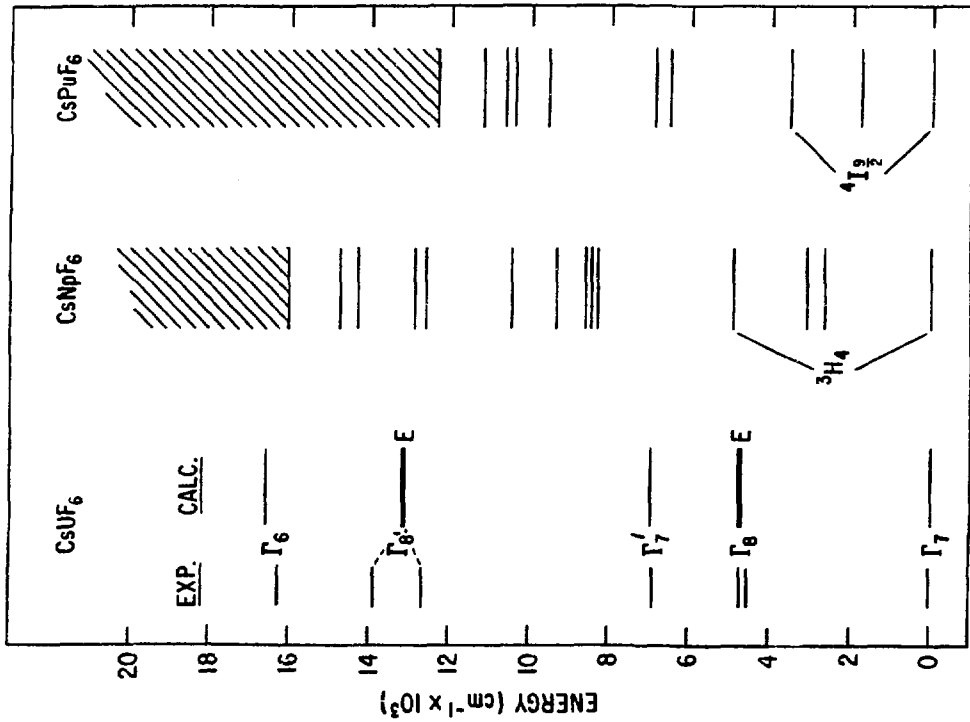


FIG. 9.

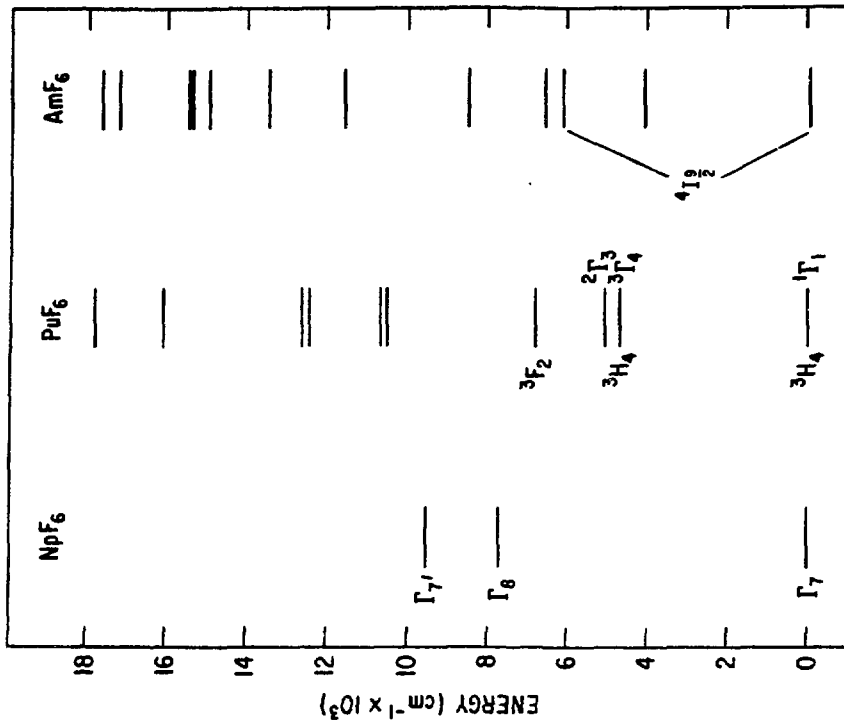


FIG. 10.